

An $\dot{f}(f)$ -frequency dynamics algorithm for gravitational waves

Maurice H. P. M. van Putten ^{*} and Abhinanda Sarkar [†]

Massachusetts Institute of Technology, Cambridge, MA 02139

Abstract

Coalescence of low mass compact binaries of neutron stars and black holes are primary burst sources for LIGO and VIRGO. Of importance in the early stages of observations will be the classification of candidate detections by source-type. The diversity in source parameters and serendipity in any new window of observations suggest to consider model-independent detection algorithms. Here a frequency dynamics algorithm is described which extracts a trajectory in the $\dot{f}(f)$ -plane from the noisy signal. The algorithm is studied in simulated binary coalescence. Robust results are obtained with experimental noise data. Experiments show the method to be superior to matched filtering in the presence of model imperfections.

I. INTRODUCTION

This millennium will mark the beginning of gravitational wave astronomy with the broad band observatories LIGO [1] and VIRGO [2]. This opens up new opportunities to probe strongly gravitating processes in the coalescence of binaries and the birth of neutron stars or black holes [3–5]. The late stages of spiral infall of a neutron star may show interesting new physics, for example, in association with tidal break-up around a companion black hole, where the onset will provide constraints on the density of neutron star matter. There may also be surprises. Advanced LIGO is expected to see events up to a Gpc [4,5], and might detect correlations or anti-correlations of gravitational radiation with cosmological γ -ray bursts. The early stages of observations will be focused on verification of potential gravitational wave signals and identification of source by type. In view of the diversity of source parameters and serendipity in any new window of observations, it is of interest to consider model-independent detection algorithms. These algorithms are expected to compare well with matched filtering, anticipating the inevitable model imperfections in both the wave-forms and the instrumentation noise.

Early evolution of a binary of two stars of mass M_1 and M_2 with orbital period P is

^{*}mvp@schauder.mit.edu

[†]sabhinan@in.ibm.com

well-described by quasi-Newtonian evolution in the point-particle limit, whose luminosity \mathcal{L}_{GW} in gravitational wave emissions in the theory of general relativity is given by the Peter and Mathews' formula [6]

$$\mathcal{L}_{GW} \sim \frac{32}{5} (\omega \mathcal{M})^{10/3} F(e) \quad (1)$$

in geometrized units with $G = c = 1$, where $\omega = 2\pi/P$ denotes the orbital angular velocity, $F(e)$ accounts for an orbital ellipticity e and $\mathcal{M} = (M_1 M_2)^{3/5}/(M_1 + M_2)^{1/5}$ denotes the chirp mass. This is accompanied by a gradual rise in the orbital frequency $f_{orb} = 1/P$:

$$\dot{f}_{orb} = \frac{96}{5} (2\pi)^{8/3} \mathcal{M}^{5/3} f_{orb}^{11/3}. \quad (2)$$

The predicted luminosity of 3.2×10^{33} ergs/s agrees with the observed rate of change 2.40×10^{-12} in the orbital period of about eight hours in the Hulse-Taylor binary system with neutron star masses $M_1 = 1.42 M_\odot$ and $M_2 = 1.4 M_\odot$ [7]. This strong frequency-luminosity relationship suggests to plot the evolution of a candidate source as a trajectory in the $\dot{f}(f)$ -plane as the output of a detection algorithm. In doing so, we focus on burst sources whose gravitational waves show appreciable dynamics in their frequencies. This, in contrast to periodic sources, e.g.: rapidly spinning neutron stars [8,9], which we regard as a separate class of sources in regards to detection algorithms. Binary coalescence of compact objects, then, shows an initial branch $\dot{f} \propto f^{11/3}$ indicative of the general relativistic relationship $\mathcal{L}_{GW} \propto f^{10/3}$. These trajectories terminate on the f -axis at the quasi-normal mode frequency f_{QNR} of a final black hole. For the expected low mass black holes $M \leq 10 M_\odot$ in compact binaries, $f_{QNR} \sim 2800(10 M_\odot/M)$ is beyond the (advanced) LIGO sensitivity range of about (20-1600Hz) 40-800Hz, however. The transition which connects the chirp to the final black hole state remains highly uncertain - here the gravitational radiation emission process is most nonlinear and potentially most interesting. For black hole-black hole coalescence, the transition from chirp to a common horizon envelope state should be smooth, may be very luminous [4] and more frequent [10] than neutron star-black hole coalescences [11-13]. In neutron star-black hole coalescence, on the other hand, an intermediate black hole-torus state is expected if the black hole spins rapidly [14]. This state is expected to be quiescent in its gravitational wave emissions, while luminous in emissions by the black hole in contact with the magnetic field of the torus [15]. This predicts an anti-correlation between gravitational wave-emissions and γ -ray bursts from this type of catastrophic events [16]. Alternatively, gravitational radiation is expected in accretion induced collapse of a white dwarf into a neutron star or black hole due to a bar mode instability [17], or the collapse of a young massive star [18,19], in which the relationship between \dot{f} and f is even more uncertain. If the collapse stalls with the formation of a neutron star, we might witness a negative branch $\dot{f} < 0$ due to spin-down by gravitational wave emissions. It becomes potentially useful, therefore, to plot transient gravitational wave emissions as trajectories in the $\dot{f}(f)$ -plane when classifying candidate detections by source-type [20]. As gravitational wave-emissions are not expected to be significantly beamed, observations such as these by advanced LIGO

can obtain definite evidence of γ -ray burst progenitors and their population statistics which are not otherwise available.

Here we describe an algorithm which enables accurate extraction of the frequency dynamics in the gravitational wave signal. The algorithm is based on counting zero-crossings, wherefrom an instantaneous frequency $f(t)$ and frequency rate of change $\dot{f}(t)$ can be estimated as a function of observer's time t . Here the proposed algorithm is tested using simulated binary coalescence with Gaussian noise and noise recorded on the 40m LIGO test facility at Caltech. The algorithm is studied on signals of the type

$$X(t) = A(t) \cos(2\pi\Phi(t)) + \sigma\tilde{N}(t) \quad (3)$$

with amplitude $A(t) = (1-t)^{-1/4}$ and phase

$$\Phi(t) = c \left[\left(1 - (1-t)^{5/8} \right) + p \left(1 - (1-t)^{3/8} \right) \right], \quad (4)$$

where $t \in [0, 1]$ is the time normalized to the time of coalescence $t = 1$, $c = 1000$ and $p \in [0, 1]$ is a model parameter: $p = 0$ in the Newtonian approximation and $p = 0.6038$ in the 1PN approximation when $M_1 = M_2$ [21]. The noise process $\tilde{N}(t)$ is normalized such that σ controls the signal-to-noise ratio. All simulations are for data strings of a total of $N = 10,000$ samples at $t_n = n\Delta t$ ($n = 1, 2, \dots, N$). The instantaneous frequency $f(t)$ is given by $d\Phi(t)/dt$ and $d^2\Phi(t)/dt^2$ denotes its rate of change $\dot{f}(t)$ with respect to time. The dimensionless rate of change of the period, $f^{-2}\dot{f}$, expresses inversely the number of periods at a frequency f , which is of the order of a few hundred in the experiments reported below (final time $t \sim 0.97$).

II. DESCRIPTION OF THE ALGORITHM

Consider the instantaneous frequency $f(t)$ as a finite time-series for $t \in [a, b]$. We begin with a partition of $[a, b]$ into N adjacent subwindows (bins) $[s_{i-1}, s_i]$ with centers at $t_i = (s_{i-1} + s_i)/2$. Linear approximations $f(t) \sim \alpha_i + \beta_i t$ ($s_{i-1} < t < s_i$) are then obtained by estimates of the coefficients α_i and β_i from the noisy data $X(t)$ in each subwindow i . The number of periods in the i -th subwindow, for example, is $\int_{s_{i-1}}^{s_i} f(t) dt = \alpha_i \delta + \beta_i t_i \delta + O(\delta^3)$, where $\delta = s_i - s_{i-1}$.

Let $Z_S(s_{i-1}, s_i)$ denote the number of zero-crossings of the true signal $S(t)$ in the subwindow $[s_{i-1}, s_i]$. Then $Z_S(s_{i-1}, s_i)$ differs from $2 \int_{s_{i-1}}^{s_i} f(t) dt$ by at most one. In view of $f(t) = d\Phi(t)/dt$, our algorithm hinges on the approximation

$$Z_S(s_{i-1}, s_i) \sim 2\delta\alpha_i + 2\delta\beta_i t_i. \quad (5)$$

The number of zero-crossings in the noisy data $(X(u_0), X(u_1), \dots, X(u_k))$ in $[s_{i-1}, s_i]$ will be denoted by $Z_X(s_{i-1}, s_i)$, where the u_j denote the discrete sampling times provided by the AD-converter (16 bit resolution, 10kHz). The $X(u_j)$ have expectation values $S(u_j)$ and

variance σ^2 . The 10kHz-sampling frequency is assumed to be sufficiently high such that the true signal agrees with the zero-crossings of its linear interpolant based on the $S(u_j)$. In terms of the indicator function, I , defined by $I(P) = 1$ if P is true and $I(P) = 0$ if P is false, we have

$$Z_S(s_{i-1}, s_i) = \sum_1^k I[S(u_{j-1})S(u_j) < 0], \quad Z_X(s_{i-1}, s_i) = \sum_1^k I[X(u_{j-1})X(u_j) < 0]. \quad (6)$$

The probability p_j that the observed signal $X(u_j)$ and its expectation (the true signal) $S(u_j)$ have the same sign can be easily computed. Suppose that $S(u_j) > 0$. Then, we have

$$P[X(u_j) > 0] = P[(X(u_j) - S(u_j))/\sigma > -S(u_j)/\sigma] = 1 - F[-S(u_j)/\sigma] = F[S(u_j)/\sigma], \quad (7)$$

where F is the probability distribution of the noise process $\tilde{N}(t)$, which is assumed to be symmetric about zero. Similarly when $S(u_j) < 0$, we find $P[X(u_j) < 0] = F[-S(u_j)/\sigma]$. It follows that $p_j = F[|S(u_j)|/\sigma]$, whereby

$$P[I[X(u_{j-1})X(u_j) < 0] \neq I[S(u_{j-1})S(u_j) < 0]] = p_{j-1}(1 - p_j) + p_j(1 - p_{j-1}). \quad (8)$$

Consider, then, $R_i = \min_j |S(u_j)|/\sigma$, as a measure for the signal-to-noise ratio in the sub-window $[s_{i-1}, s_i]$. As $R_i \rightarrow \infty$, $\min_j p_j \rightarrow 1$. We then have for the expectation E and the variance V the limits

$$\lim_{R_i \rightarrow \infty} E[Z_X(s_{i-1}, s_i)] = Z_S(s_{i-1}, s_i), \quad V[Z_X(s_{i-1}, s_i)] = 0. \quad (9)$$

Hence, for large signal to noise ratios, we recover $Z_X(s_{i-1}, s_i) \sim 2\delta\alpha_i + 2\delta\beta_i t_i$.

Estimates α_i for $f(t_i)$ and β_i for $\dot{f}(t_i)$ can be calculated by linear regression. Define (as is usual in such regressions, see, e.g. [22]) the L^2 error

$$Q(\alpha_i, \beta_i) = \sum_1^N (Z_X(s_{i-1}, s_i) - (2\delta\alpha_i + 2\delta\beta_i t_i))^2. \quad (10)$$

Let $\hat{\alpha}_i, \hat{\beta}_i$ minimize $Q(\alpha, \beta)$. The regression estimates of the instantaneous frequency $f(t_i)$ and its rate of change $\dot{f}(t_i)$ are $\hat{\alpha}_i$ and $\hat{\beta}_i$ respectively. As these are obtained simultaneously, the \dot{f} are on equal par with f , rather than being their derivatives. Standard regression theory allows us to compute error boxes in these estimates. Note that the method amounts to an approximation of the time-series $f(t)$ by a piecewise linear, and generally discontinuous function.

The method may be optimized by modifying the present L^2 norm in the error function to curve fitting, e.g.: different weights on f and \dot{f} . Initial experiments indicate that the method can be implemented with adaptive window sizes, which may improve its efficiency when the dynamic range in the frequency $f(t)$ is large.

Because only the pattern of zero-crossings is measured, the algorithm targets precisely the underlying gravitational wave frequency-luminosity relationship of the source, as exemplified in binary coalescence. The algorithm suppresses the amplitude of the signal, and hence it is robust to size fluctuations in the signal. Likewise, reference to the underlying cosine functions is weak. In fact, any 2π -function with two roots in each period can replace the cosine function in (1).

III. NOISE DEPENDENCE

The frequency dynamics algorithm has been tested in simulated binary coalescence using the Newtonian model of spiral in ($p = 0$) with Gaussian noise and the instrumental noise from the 40m-LIGO test facility at Caltech. The chirp extends over $t = [0, 0.97]$, wherein the number of periods at a given frequency $f(t)$ decreases from above 400 to below 200. Figure 1 shows the results for both cases.

The algorithm obtains higher accuracy with the 40m-LIGO noise than with Gaussian noise when the variance is high. We believe that the reason for this lies in the high-degree of dependence in the noise from the LIGO prototype. The first-order autocorrelations from 40m-LIGO noise were of the order of 0.8. There were, on average, 15 zero-crossings per 100 recordings of the pure noise process. This is much smaller than the 50 or so zero crossings obtained for white noise of the same length. Thus the LIGO noise contributes far fewer “false crossing” due to noise as opposed to signal. This will be the case for all noise with low-frequency components in the spectrum. In such cases, our algorithms performs even better than it would with white noise. To make the last point more precise, consider a Gaussian process with a first order autocorrelation of ρ . If we observe a sequence of length N from such a process the expected number of zero-crossings is

$$\frac{(N-1)}{2} \left(1 - \frac{2}{\pi} \tan^{-1} \frac{\rho}{\sqrt{1-\rho^2}} \right)$$

For ρ of 0.8, as in the LIGO case, we would expect approximately 20 zero crossings per 100 recordings. Of course, the LIGO noise from the Caltech prototype is not pure Gaussian, but the principle is the same.

IV. COMPARISON WITH MATCHED FILTERING

Optimal application of matched filtering requires accurate models of the system to be detected and the noise of the detector. Both aspects of prior knowledge are critical and must be described in a low number of parameters, lest matched filtering becomes unstable. Detection of gravitational waves from forementioned candidate sources poses a number of uncertainties which may enter as model imperfections (e.g., size of neutron stars [23]). These imperfections can give rise to woefully wrong results when the true signal is not contained in the model for any choice of its parameters. It becomes of interest, therefore, to compare the model-independence aspect of the frequency dynamics algorithm with the sensitivity of matched filtering to these imperfections. The comparison would be complete with an additional on noise type and intensity which, however, falls outside the scope of this work. The comparison is made using the post-Newtonian model in the 1PN approximation as the true signal ($p = 0.6038$), while applying matched filtering assuming the Newtonian model given by $p = 0$. This mismatch of model to true signal is used here to simulate other model imperfections, such as due to the finite size of the objects.

Thus, the matched filtering model is perfect in case of $p = 0$, and becomes imperfect as $p \neq 0$. It is expected that matched filtering will outperform the frequency dynamics algorithm for $p = 0$, and vice-versa for certain larger values of $p > 0$. The comparison is made quantitative using a mean absolute relative error (MARE), expressed as a percentage, in the estimated frequencies by comparison with the known signal input:

$$\text{MARE} = \frac{100}{N} \sum_1^N \frac{|\hat{f}(t_i) - f(t_i)|}{f(t_i)} \quad (11)$$

Using a small Monte Carlo study, the comparison is made at three levels of additive Gaussian white noise. Figure 2 shows the results of this comparison study, where each reported MARE is the average of 200 simulations.

V. CONCLUSIONS

The trajectory in the $\dot{f}(f)$ -plane of a burst of gravitational radiation is expected to provide a signature of the source. This is anticipated from the strong - possibly characteristic - coupling between the frequency and the luminosity of its gravitational wave emissions. Binary coalescence, for example, shows the characteristic chirp $\dot{f} \propto f^{\alpha+1/3}$ associated with a luminosity $\mathcal{L}_{GW} \propto f^\alpha$, where $\alpha = 10/3$ in general relativity in the point-particle limit. Other burst sources of gravitational radiation may have different frequency dynamics (e.g.: different α 's). We have described a nonparametric (model-free) frequency dynamics algorithm to obtain an accurate plot of the trajectory in the $\dot{f}(f)$ -plane. It is based on zero-crossings in the gravitational wave signal, to extract these trajectories in the presence of noise. The method is robust against non-Gaussian additive noise and amplitude variations. The method shows good results at appreciable chirp rates and different types of noise. Even when the signal-to-noise level is low (down to about 2 in our experiments), we can still recover the distinctive curve of the frequency dynamics when \dot{f} is high. The estimation appears to be much more accurate for LIGO noise than for Gaussian noise when the variance is high. We believe that the reason for this lies in the high-degree of dependence in the noise from the LIGO prototype, which suppresses “false zero-crossings” generated by the noise. This will be the case for all noise with low-frequency components in the spectrum. In such cases, our algorithm performs even better than it would with white noise. The frequency dynamics algorithm has been compared with matched filtering, and shown to be superior in the presence of model imperfections. This is particularly relevant in searches for unanticipated burst sources.

The present experiments indicate that the algorithm should perform well in extracting the frequency dynamics in the gravitational waves. Future experiments are desirable at very low signal-to-noise levels, to study the detection limit for transient sources with the present algorithm.

Acknowledgements. This research received partial support from NASA grant NAG5-7012, LIGO and an MIT Reed Award. The authors are grateful to R. Weiss for constructive comments, and A. Lazzarini for kindly providing the LIGO data.

Figure Captions

Figure 1. The $\dot{f}(f)$ -diagram of simulated binary coalescence in the Newtonian approximation, extracted by the frequency dynamics algorithm in the presence of noise at a signal-to-noise ratio of about 4 ($s = \sigma = 0.25$). The horizontal axis shows the frequency f [Hz] and the vertical axis its time rate of change df [Hz/s]. The top window shows the results with Gaussian noise, and the lower window shows the results with the instrumental noise from the 40m-LIGO test facility at Caltech. The crosses in the right windows denote horizontal and vertical errors obtained from the linear regression estimates. The results indicate that the method improves when the noise is correlated. At higher frequencies, the results are similar due to a larger instantaneous signal-to-noise ratio.

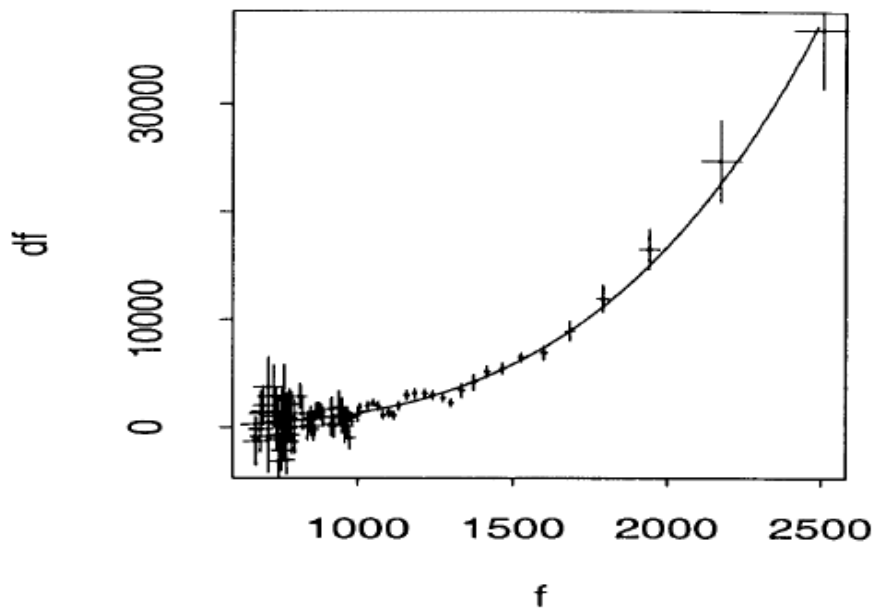
Figure 2. Experiments on model-independence in terms of the normalized error MARE on the frequency, obtained by the frequency dynamics algorithms (lines) and matched filtering (dashed) at three different variances $\sigma^2 = 0.01, 0.15, 0.25$. The comparisons are made for three different signals, parametrized by the value of p (horizontal axis). Matched filtering is performed with model assumption $p = 0$, hence $p \neq 0$ in the signal simulates a model imperfection. The results show that the frequency dynamics algorithm outperforms matched filtering in the presence of such appreciable model imperfections, with MARE approaching a constant.

References

- [1] Abramovici A. *et al.*, *Science*, **256**, 325 (1992).
- [2] Bradaschia C. *et al.*, *Phys. Lett. A*, **163**, 15 (1992).
- [3] Cutler C. *et al.*, *Phys. Rev. Lett.*, **70**, 2984 (1993).
- [4] Thorne K.S., gr-qc/9506086 (1995); *ibid.* gr-qc/9506084 (1995).
- [5] Shutz B.F., gr-qc/9911034 (1999).
- [6] Peter & Mathews, *Phys. Rev.*, **131**, 435 (1963).
- [7] Hulse R.A. & Taylor J.H., *ApJ.*, **195**, L51 (1975); Taylor J.H. and Weisberg J.M., *ApJ.*, **253**, 908 (1982); Weisberg J.M. and Taylor J.H., *Phys. Rev. Lett.*, **52**, 1348 (1984).
- [8] Shutz B.F., *in 2nd Workshop on Gravitational Wave Analysis*, M. Davier & P. Hello eds., Orsay, France (1997), p133.
- [9] Bildsten L., *ApJ.*, **501**:L89 (1998).
- [10] Portugies Zwart S.F. and McMillain S.F.W., *ApJ.*, **503**:L17 (2000).
- [11] Phinney E.S., *ApJ.*, **380**:L17 (1991).
- [12] Narayan R., Piran T.& Shemi A., *ApJ.*, **379**:L17 (1991).
- [13] Hello P., *in 2nd Workshop on Gravitational Wave Analysis*, M. Davier & P. Hello eds., Orsay, France (1997), p87.
- [14] Paczynski B., *Acta Atron.*, **41**:257 (1991).
- [15] van Putten M.H.P.M., *Phys. Rev. Lett.*, **84**(17):3752 (2000).
- [16] van Putten M.H.P.M., *Science*, **284**:115 (1999).

- [17] Usov V.V., *Nature*, **357**:472 (1992).
- [18] Woosley S.E., *ApJ.*, **405**:273 (1993).
- [19] Paczyński B., **ApJ.**, **494**:L45 (1998).
- [20] van Putten M.H.P.M., *in 8th Marcel Grossman Meeting*, Ruffini & Piran (eds.), Jerusalem (World Scientific, Singapore, 1998), p768.
- [21] Wagoner R.V. & Will C.W., *ApJ*, **210**:764 (1976); *ibid.* **215**:984 (1977); Blanchet L., Damour T., Iyer B.R., Will C.W. & Wiseman A.G., *Phys. Rev. Lett.*, **74**(18): 3515 (1995); Blanchet L., Damour T., Iyer B.R., *Phys. Rev. D.*, **51**(10):5360 (1995).
- [22] Venables W.N. & Ripley B.D., “Modern Applied Statistics with S-Plus,” 2nd edition (Springer, New York, 1997).
- [23] Blanchet L., *in 2nd Workshop on Gravitational Wave Analysis*, M. Davier & P. Hello eds., Orsay, France (1997), p67.

s=0.25, Gaussian



s=0.25, LIGO

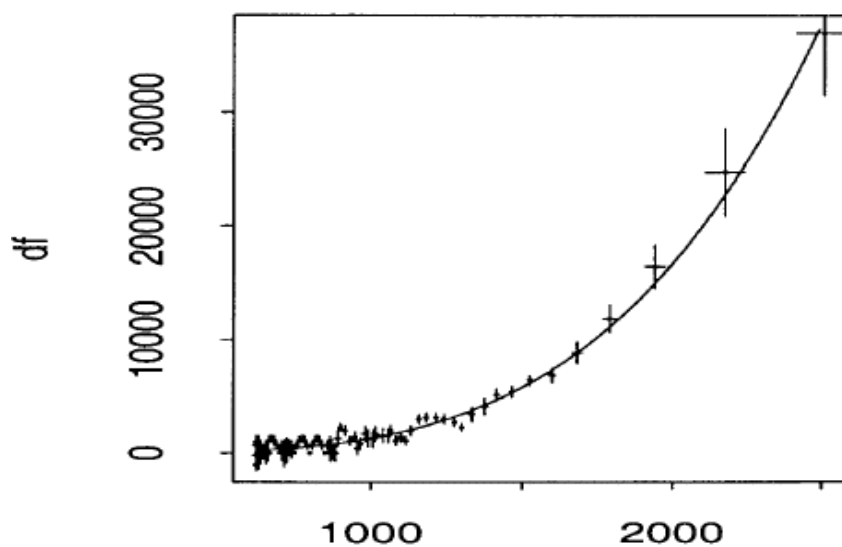


Figure 1.

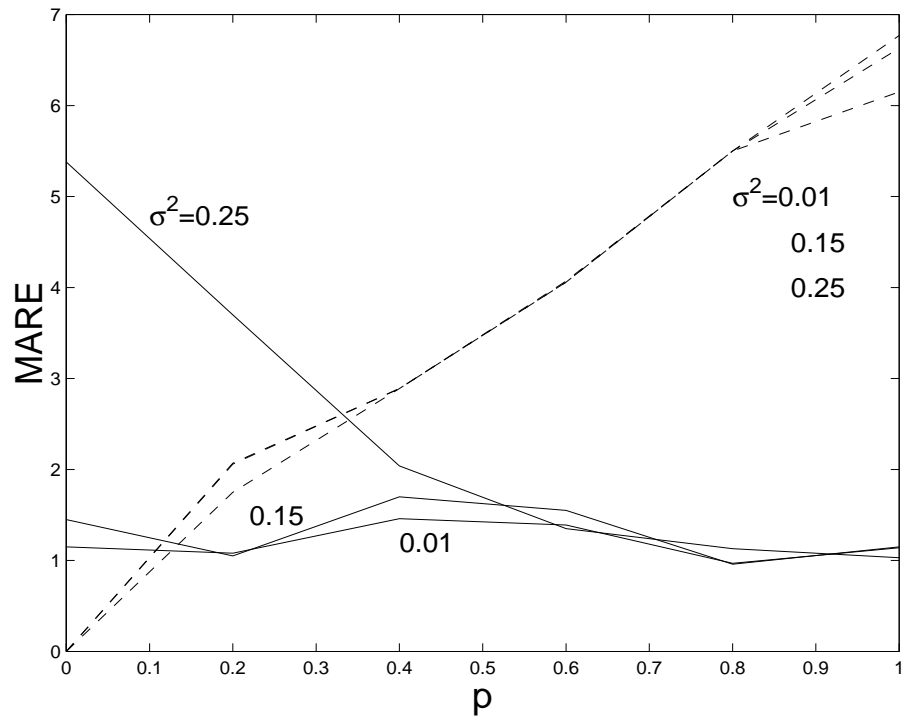


Figure 2.